

Einstein-de Haas Effect in Dipolar Bose-Einstein Condensates

Yuki Kawaguchi¹, Hiroki Saito¹, and Masahito Ueda^{1,2}

¹*Department of Physics, Tokyo Institute of Technology,
2-12-1 Ookayama, Meguro-ku, Tokyo 152-8551, Japan*

²*ERATO, Japan Science and Technology Corporation (JST), Saitama 332-0012, Japan*

(Dated: December 22, 2019)

General properties of the order parameter for a dipolar spinor multicomponent Bose-Einstein condensate is discussed based on symmetries of the interactions. An initially spin-polarized dipolar condensate is shown to dynamically generate a new type of non-singular vortex via spin-orbit interactions, reminiscent of the Einstein-de Haas effect in ferromagnets.

PACS numbers: 03.75.Mn,03.75.Nt,03.75.Kk,03.75.Lm

Realization of a Bose-Einstein condensate (BEC) of ^{52}Cr [1, 2] marks a major development in degenerate quantum gases in that the interparticle interaction via magnetic dipoles is much larger than those in the other spinor BECs of Alkali atoms. The long-range nature and anisotropy of the dipolar interaction pose challenging questions concerning the stability and superfluidity of the BEC [3, 4, 5, 6, 7, 8, 9, 10]. The ground state of the ^{52}Cr atom has a total electronic spin of three and a nuclear spin of zero, and therefore the ^{52}Cr BEC has seven internal degrees of freedom. The interplay between dipolar and spinor interactions makes the order parameter of this system highly non-trivial [11, 12, 13]. Moreover, the dipole interaction couples the spin and orbital angular momenta so that an initial magnetization of the system causes the gas to rotate mechanically (the “Einstein-de Haas effect” [14]) or, conversely, a solid-body rotation of the system leads to its magnetization (the “Barnett effect” [15]).

The aim of this Letter is to investigate the Einstein-de Haas and Barnett effects in a spin-3 BEC system and to derive the symmetry of the order parameter from general principles. We also study the dynamic formation of spin texture using numerical simulations of the seven-component non-local mean-field theory which takes into account short-range (van der Waals) interactions and magnetic dipole-dipole interactions subject to a trapping potential and external magnetic field.

Let us first investigate general symmetry properties of the order parameter by discussing two fundamental symmetries of the dipolar interaction between two magnetic dipole moments $\boldsymbol{\mu}_1 = g\mu_B \hat{\mathbf{s}}_1$ and $\boldsymbol{\mu}_2 = g\mu_B \hat{\mathbf{s}}_2$, where g is the electron g -factor, μ_B is the Bohr magneton, and $\hat{\mathbf{s}}_1$ and $\hat{\mathbf{s}}_2$ are the spin operators. The interaction between the two magnetic dipoles located at \mathbf{r}_1 and \mathbf{r}_2 is given by

$$\hat{v}_{dd}(\mathbf{r}_{12}) = c_{dd} \frac{(\hat{\mathbf{s}}_1 \cdot \hat{\mathbf{s}}_2) - 3(\hat{\mathbf{s}}_1 \cdot \mathbf{e}_{12})(\hat{\mathbf{s}}_2 \cdot \mathbf{e}_{12})}{r_{12}^3}, \quad (1)$$

where $\mathbf{r}_{12} \equiv \mathbf{r}_1 - \mathbf{r}_2$, $\mathbf{e}_{12} \equiv \mathbf{r}_{12}/r_{12}$, and $c_{dd} = \mu_0(g\mu_B)^2/4\pi$ with μ_0 being the magnetic permeability of the vacuum. The dipole interaction is invariant under simultaneous rotation in spin and coordinate spaces about

an arbitrary axis, say the z -axis, so that the projected total angular momentum operator $\hat{S}_z + \hat{L}_z$ on that axis commutes with \hat{v}_{dd} , where $\hat{\mathbf{S}} = \hat{\mathbf{s}}_1 + \hat{\mathbf{s}}_2$ is the total spin angular momentum operator and $\hat{\mathbf{L}}$ is the relative orbital angular momentum operator. The other symmetry of the dipolar interaction is that it is invariant under the transformation $\mathbf{P}_z e^{-i\pi\hat{S}_z}$, where $\mathbf{P}_z : (x, y, z) \rightarrow (x, y, -z)$ and $e^{-i\pi\hat{S}_z} : (\hat{S}_x, \hat{S}_y, \hat{S}_z) \rightarrow (-\hat{S}_x, -\hat{S}_y, \hat{S}_z)$. Thus, the eigenvalues of the following operators are conserved by the dipole interaction:

$$\hat{S}_z + \hat{L}_z \quad \text{and} \quad \mathbf{P}_z e^{-i\pi\hat{S}_z}. \quad (2)$$

A crucial observation here is that these operators also commute with the short-range interactions. Thus if the confining potential is axisymmetric, the simultaneous eigenfunctions of the two operators (2) can serve to classify the two-body wave function.

Constructing a many-body wave function by directly applying these symmetry considerations is quite complicated since the system has many degrees of freedom. However, insight for substantial simplification can be gained by considering the case of a ferromagnet in which dipole moments are localized at lattice sites and thus the degrees of freedom of the system are reduced to those of center-of-mass motion and the solid-body rotation around it. Consequently, spin relaxation of the system leads to a solid-body rotation of the ferromagnet – an effect known as the “Einstein-de Haas effect” [14]. Analogous considerations can be applied to a BEC because almost all atoms occupy a single-particle state and, therefore, the degrees of freedom of the system can be represented by those of the order parameter. We may thus expect the Einstein-de Haas effect to emerge in the dipolar BEC system.

It follows from the symmetry considerations of the dipolar interaction described above that the order parameter of dipolar spinor BECs can be classified by the eigenvalues of the operators (2). In general, the order parameter of a BEC can be defined as the eigenfunction corresponding to the macroscopic eigenvalue of the reduced single-particle density operator. Let the order

parameter be denoted as $\psi_\alpha(\mathbf{r})$ the norm of which is assumed to be N , the number of condensate atoms. Then a dipolar spinor order parameter can be expanded in terms of the eigenstates of the operators (2) as

$$\psi_\alpha(r, \phi, z, t) = \sum_{J=0, \pm 1, \dots} \sum_{p=\pm 1} e^{i(J-\alpha)\phi} \eta_{\alpha J p}(r, z, t), \quad (3)$$

where J and p denote the eigenvalues of $\hat{S}_z + \hat{L}_z$ and $P_z e^{-i\pi\hat{S}_z}$, respectively, and $\eta_{\alpha J p}$ is the complex eigenfunction of P_z satisfying $P_z \eta_{\alpha J p} = p(-1)^\alpha \eta_{\alpha J p}$. As mentioned earlier the short-range interaction Hamiltonians also commute with the operators (2) and, therefore, components with different J or p do not mix if the trapping potential is axisymmetric.

We now discuss the dynamic formation of spin texture in a dipolar BEC. The order parameter obeys the following set of the non-local Gross-Pitaevskii equations:

$$\begin{aligned} i\hbar \frac{d\psi_\alpha(\mathbf{r})}{dt} = & \left[-\frac{\hbar^2 \nabla^2}{2M} + g\mu_B B_{\text{ext}} \alpha + U_{\text{trap}}(\mathbf{r}) \right] \psi_\alpha(\mathbf{r}) \\ & + \sum_{\beta \alpha' \beta'} \sum_{S=0}^{2s} g_S \langle \alpha \beta | \mathcal{P}_S | \alpha' \beta' \rangle \psi_\beta^*(\mathbf{r}) \psi_{\alpha'}(\mathbf{r}) \psi_{\beta'}(\mathbf{r}) \\ & + \sum_{\mu=x,y,z} \sum_{\beta} B_{\text{eff}}^\mu(\mathbf{r}) (g\mu_B s_{\alpha\beta}^\mu) \psi_\beta(\mathbf{r}), \end{aligned} \quad (4)$$

where M is the atomic mass, B_{ext} is the external magnetic field which is assumed to be applied in the z direction, and $U_{\text{trap}}(\mathbf{r})$ is the trapping potential. The second line in Eq. (4) represents the short-range interaction, where the strength of the interaction is characterized in terms of the s -wave scattering length a_S for a total spin S as $g_S = 4\pi\hbar^2 a_S / M$. Here \mathcal{P}_S is the operator that projects the wave function into Hilbert space with a definite total spin and is expressed in terms of the Clebsch-Gordan coefficients $\langle s\alpha s\beta | S M_S \rangle$ as $\langle \alpha \beta | \mathcal{P}_S | \alpha' \beta' \rangle = \sum_{M_S=-S}^S \langle s\alpha s\beta | S M_S \rangle \langle S M_S | s\alpha' s\beta' \rangle$ [16].

The last line in Eq. (4) represents the dipole-dipole interaction, where $s^{x,y,z}$ are the spin- s matrices, and

$$\begin{aligned} B_{\text{eff}}^\mu(\mathbf{r}) \equiv & \frac{c_{\text{dd}}}{g\mu_B} \sum_{\nu} \int d\mathbf{r}' \frac{\delta_{\mu\nu} - 3e^\mu e^\nu}{|\mathbf{r} - \mathbf{r}'|^3} \\ & \sum_{\alpha' \beta'} \psi_{\alpha'}^*(\mathbf{r}') s_{\alpha' \beta'}^\nu \psi_{\beta'}(\mathbf{r}') \end{aligned} \quad (5)$$

is an effective magnetic field at \mathbf{r} produced by the surrounding magnetic dipoles, with $\mathbf{e} \equiv (\mathbf{r} - \mathbf{r}')/|\mathbf{r} - \mathbf{r}'|$. Here we introduce the expectation value of spin matrices as $S^\mu(\mathbf{r}) = \sum_{\alpha\beta} \psi_\alpha^*(\mathbf{r}) s_{\alpha\beta}^\mu \psi_\beta(\mathbf{r})$. Calculating the time derivative of S^μ , one finds that, apart from the spinor interactions, $\mathbf{S}(\mathbf{r})$ behaves like a “classical” spin, which undergoes Larmor precession around the effective local magnetic field $\mathbf{B}_{\text{eff}}(\mathbf{r}) + B_{\text{ext}}\hat{z}$. The spin flip occurs in the region where $B_{\text{eff}}^{x,y}(\mathbf{r})$ are finite. In a homogeneous infinite system, the effective field is completely canceled

out for a polarized BEC, and the spin flip does not occur. Therefore, the Einstein-de Haas effect in a dipolar BEC is unique to non-uniform systems.

Let us now study the spin dynamics of the Einstein-de Haas effect in an experimentally realized spin-3 ^{52}Cr BEC system. We consider a situation in which a stable spin-polarized BEC in the lowest spin sublevel $\alpha = -3$ is produced in a strong magnetic field as in the experiments [1, 2], and then the magnetic field is suddenly decreased to B_{ext} . The initial state is calculated by applying the method of imaginary-time propagation to Eq. (4) by treating $\psi_{-3}(\mathbf{r})$ as a scalar order parameter. We have performed three-dimensional simulations of Eq. (4) with seven spin components by using the Crank-Nicolson method. The scattering lengths of ^{52}Cr are reported to be $a_6 = 112$, $a_4 = 58$, and $a_2 = -7$ in units of Bohr radius [17]. The value of a_0 is unknown and we estimate it by using the van der Waals coefficient C_6 given in Ref. [17] as $a_0 \sim (C_6 M/m_e)^{1/4} = 91$, where m_e is the electron mass. Since we are interested in spin dynamics from the fully spin-polarized state, the short-range interaction is dominated by a_6 and a_4 , and the value of a_0 does not qualitatively affect the results discussed below.

We assume $N = 10^5$ atoms trapped in an axisymmetric potential $U_{\text{trap}}(\mathbf{r}) = (1/2)M\omega^2(r^2 + z^2/\lambda^4)$ with $\omega = 2\pi \times 820$ Hz. The typical ratio of dipolar interaction to short-range interaction is $s^2 c_{\text{dd}}/g_6 \simeq 0.03$, with $s = 3$. In a spherical trap, the number density at the trap center is $n \simeq 7 \times 10^{20} \text{ m}^{-3}$ and the dipole-dipole interaction energy $s^2 c_{\text{dd}} n$ becomes the same order of magnitude as the Zeeman energy for $B_{\text{ext}} \simeq 0.1 \text{ mG}$. Hence, the spin-flip rate becomes significant for $|B_{\text{ext}}| \lesssim 1 \text{ mG}$. In the following, we first consider $B_{\text{ext}} = 0$ and $\lambda = 1$, and then discuss the effect of the external magnetic field and that of the trap geometry.

Figure 1 shows the results for $B_{\text{ext}} = 0$ and $\lambda = 1$. In Fig. 1(a), we plot the population of each spin state $N_\alpha/N \equiv \int d\mathbf{r} |\psi_\alpha|^2 / N$ as a function of ωt . We see that N_{-2}/N first increases rapidly and then the components with $\alpha \geq -1$ grow. Figures 1(b), (c), and (d) show the three-dimensional plots of ψ_{-3} , ψ_{-2} , and ψ_{-1} at $\omega t = 2$, respectively, where the values of $|\psi_\alpha|^2$ are scaled by N/a_{ho}^3 with a_{ho} being the harmonic oscillator length $\sqrt{\hbar/2M\omega}$. The order parameters indeed show the symmetries discussed earlier on generic grounds: ψ_{-2} has a phase winding number of 1 and the node plane at $z = 0$, and ψ_{-1} has a winding number of 2 and reflection symmetry with respect to the xy -plane. Since the order parameters of different spin components are connected with each other, the Einstein-de Haas effect in a trapped BEC produces a non-singular vortex, or a skyrmion. The effective magnetic field (5) at $\omega t = 0$ and the spin vector at $\omega t = 2$ are plotted in Fig. 2. The whirling patterns of the spin texture in Figs. 2(b) and (c) are due to Larmor precession around the local magnetic field shown in Fig. 2(a). Since the local magnetic field points outward for $z > 0$

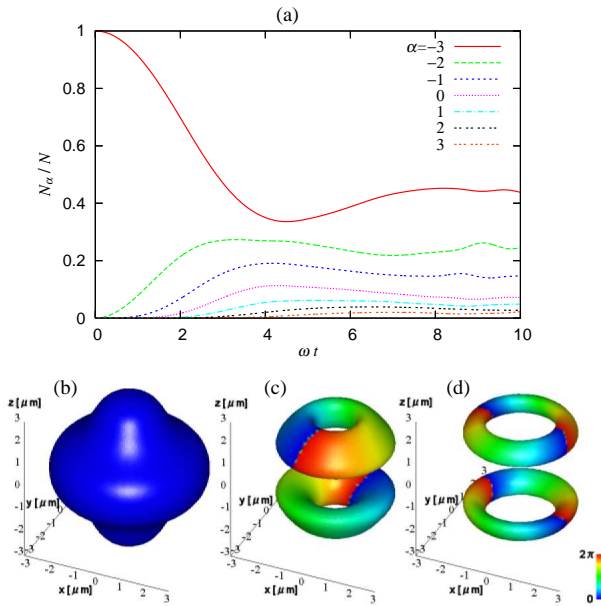


FIG. 1: (Color) (a) Relative population $N_\alpha/N = \int dr |\psi_\alpha|^2/N$ of each magnetic sublevel α versus ωt for $B_{\text{ext}} = 0$ and $\lambda = 1$. (b)-(d) Isopycnic surfaces of (b) ψ_{-3} , (c) ψ_{-2} , and (d) ψ_{-1} at $\omega t = 2$, where $|\psi_\alpha|^2 a_{\text{ho}}^3/N = 0.0001$ for (b) and (c) and 5×10^{-5} for (d). The color on the surface represents the phase of the order parameter (see the right gauge).

and inward for $z < 0$, the senses of the whirlpools in Figs. 2(b) and (c) are opposite.

When the external magnetic field B_{ext} is applied in the positive z -direction and is much stronger than the dipole field, the spin angular momentum should be conserved because of energy conservation, and spin flip is suppressed. When $B_{\text{ext}} < 0$, spin flip can occur by converting the Zeeman energy to kinetic energy. These behaviors are demonstrated in Fig. 3(a), in which the time evolution of N_{-2}/N for $B_{\text{ext}} = \pm 1$ mG is plotted. Figures 3(b) and (c) show cross sections of $|\psi_{-2}|^2 a_{\text{ho}}^3/N$ for $B_{\text{ext}} = \pm 1$ mG at $\omega t = 8$ and $\lambda = 1$. When $B_{\text{ext}} > 0$, ψ_{-2} oscillates in time between the structure of Fig. 1(c) and that of Fig. 3(b). When the initial state is spherical, these structures are derived by the symmetry of the dipole interaction, which is expressed in terms of the rank-2 spherical harmonics Y_{2m} . The dipole field produced by $\psi_{-3}(\propto Y_{00}(\mathbf{r}))$ induces a $Y_{2-1}(\mathbf{r})$ term in ψ_{-2} (Fig. 1(c)), and similarly the $Y_{2-1}(\mathbf{r})$ term in ψ_{-2} affects itself and induces a linear combination of $Y_{2-1}(\mathbf{r})$ and $Y_{4-1}(\mathbf{r})$, resulting in Fig. 3(b). Therefore, the structure in Fig. 3(b) appears as a secondary effect of the dipole-dipole interaction. In the case $B_{\text{ext}} = -1$ mG, a similar structure as in Fig. 3(b) appears when $\omega t \lesssim 4$. However, as time advances, the domain structure shown in Fig. 3(c) develops. The domain size becomes smaller as the value of $|B_{\text{ext}}|$ increases.

Finally, we discuss the geometry dependence of the

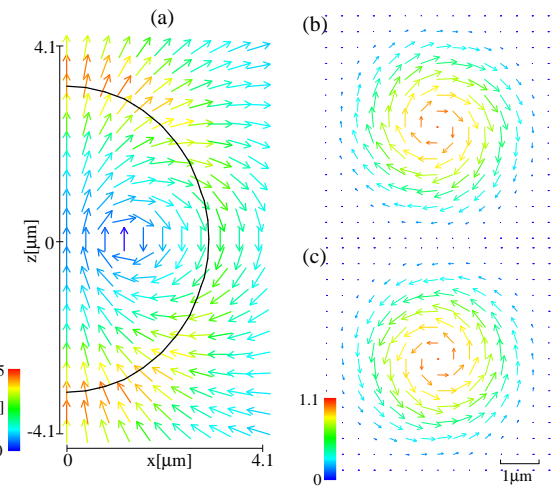


FIG. 2: (Color) (a) Dipole field at $t = 0$ for $\lambda = 1$. The solid curve shows isopycnic curve at $|\psi_{-3}|^2 a_{\text{ho}}^3/N = 0.0001$. The color of the arrows denotes the magnitude of the field. (b)(c) Spin configurations on the (b) $z = 2 \mu\text{m}$ -plane and (c) $z = -2 \mu\text{m}$ -plane at $\omega t = 2$ for $B_{\text{ext}} = 0$ and $\lambda = 0$. The length of the arrow represents the magnitude of the spin vector projected on the xy -plane and the color shows $|S|$. Note that spins tilt in a direction perpendicular to $\mathbf{B}_{\text{eff}}(\mathbf{r})$.

condensate. Figure 4 shows the dipole field $\mathbf{B}_{\text{eff}}(\mathbf{r})$ at $t = 0$ for $\lambda = 0.5$. Compared with Fig. 2(a), the z -component of the effective magnetic field is inverted around the center of the condensate. The transfer of atoms between two spin sublevels is due to the Larmor precession caused by B_{eff}^{xy} , and it occurs most efficiently when the local magnetic field in the z -direction $B_{\text{eff}}^z + B_{\text{ext}}$ vanishes. The sign of such optimized B_{ext} for BECs in spherical traps is opposite to that for BECs in pancake-shaped traps, as can be inferred from Fig. 2(a) and Fig. 4. This fact is indeed reflected in Fig. 3(a) as the difference in the field dependence of the initial peaks. Since the z -component of the dipole field is positive in most of the condensate when $\lambda = 1$ (Fig. 2(a)), the initial peak in Fig. 3(a) is larger for $B_{\text{ext}} = -1$ mG than for $B_{\text{ext}} = 1$ mG. The relation between the initial peak and B_{ext} is opposite in the case for $\lambda = 0.5$, since the z -component of the dipole field is mostly negative in the condensate (Fig. 4). In the case of a cigarette-shaped BEC, the qualitative behavior is the same as in the spherical trap.

In conclusion, we have shown that the Einstein-de Haas effect occurs in dipolar spinor Bose-Einstein condensates and that a non-singular vortex appears from an initially polarized condensate. In the course of spin-relaxation processes, different vortex structures develop, depending on the external magnetic field. In particular, in a low magnetic field (~ 1 mG) the fraction of the spin-flipped atoms ($\sim 5\%$) is large enough to be observed in Stern-Gerlach experiments.

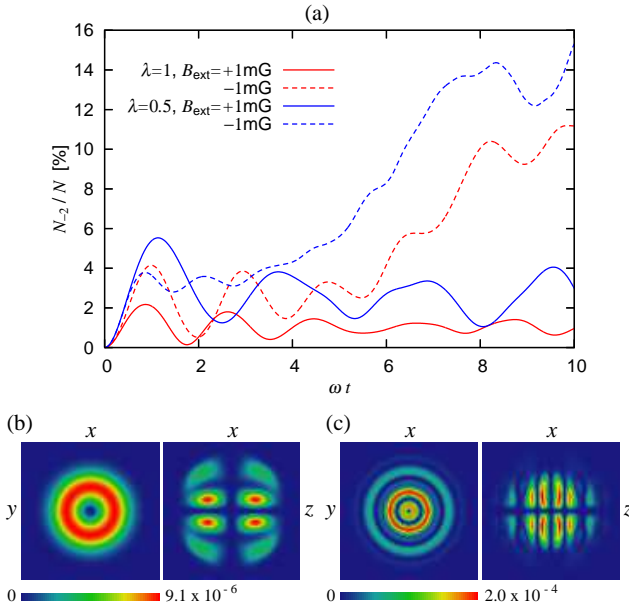


FIG. 3: (Color) (a) Population of $\alpha = -2$ sublevel versus ωt for $B_{ext} = \pm 1 \text{ mG}$ and $\lambda = 1$ and 0.5. (b)(c) Cross sections of $|\psi_{-2}|^2 a_{ho}^3 / N$ with $\lambda = 1$ at $\omega t = 8$ for (b) $B_{ext} = 1 \text{ mG}$ and (c) -1 mG . The cut surfaces are at $z = 0.7 \mu\text{m}$ (left) and $y = 0 \mu\text{m}$ (right). The size of each panel is $8.2 \times 8.2 \mu\text{m}$.

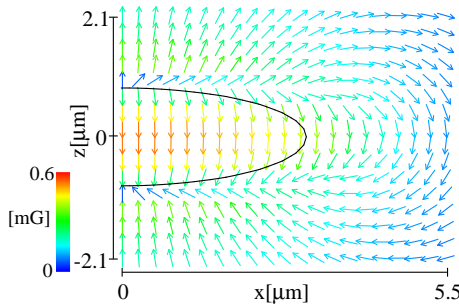


FIG. 4: (Color) Dipole field at $t = 0$ for $\lambda = 0.5$. The solid curve shows an isopycnic curve at $|\psi_{-3}|^2 a_{ho}^3 / N = 0.0005$. Note that the sign of $B_{\text{eff}}^z(\mathbf{r})$ in the condensate is opposite to that in Fig. 2(a).

This work was supported by Grant-in-Aids for Scientific Research (Grant No. 17740263, No. 17071005, and

No. 15340129) and by a 21st Century COE program at Tokyo Tech “Nanometer-Scale Quantum Physics” from the Ministry of Education, Culture, Sports, Science and Technology of Japan. YK acknowledges support by a Fellowship Program of the Japan Society for Promotion of Science (Project No. 160648). MU acknowledges support by a CREST program of the JST.

Note added. — Very recently, a preprint [18] appeared which also discusses the Einstein-de Haas effect in a dipolar BEC.

- [1] A. Griesmaier, J. Werner, S. Hensler, J. Stuhler, and T. Pfau, Phys. Rev. Lett. **94**, 160401 (2005).
- [2] J. Stuhler, A. Griesmaier, T. Koch, M. Fattori, T. Pfau, S. Giovanazzi, P. Pedri, and L. Santos, Phys. Rev. Lett. **95**, 150406 (2005).
- [3] L. Santos, G. V. Shlyapnikov, P. Zoller, and M. Lewenstein, Phys. Rev. Lett. **85**, 1791 (2000).
- [4] L. Santos, G. V. Shlyapnikov, and M. Lewenstein, Phys. Rev. Lett. **90**, 250403 (2003).
- [5] K. Góral and L. Santos, Phys. Rev. A **66**, 023613 (2002).
- [6] K. Góral, K. Rzazewski, and T. Pfau, Phys. Rev. A **61**, 051601(R) (2000).
- [7] D. H. J. O’Dell, S. Giovanazzi, and C. Eberlein, Phys. Rev. Lett. **92**, 250401 (2004).
- [8] C. Eberlein, S. Giovanazzi, and D. H. J. O’Dell, Phys. Rev. A **71**, 033618 (2005).
- [9] S. Yi and L. You, Phys. Rev. A **63**, 053607 (2001).
- [10] M. Baranov, L. Dobrek, K. Góral, L. Santos, and M. Lewenstein, Physica Scripta. **T102**, 74 (2002).
- [11] S. Yi, L. You, and H. Pu, Phys. Rev. Lett. **93**, 040403 (2004).
- [12] H. Pu, W. Zhang, and P. Meystre, Phys. Rev. Lett. **87**, 140405 (2001).
- [13] K. Gross, C. P. Search, H. Pu, W. Zhang, and P. Meystre, Phys. Rev. A **66**, 033603 (2002).
- [14] A. Einstein and W. J. de Haas, Verhandl. Deut. Physik. Gas **17**, 152 (1915).
- [15] S. J. Barnett, Phys. Rev. **6**, 239 (1915).
- [16] T.-L. Ho, Phys. Rev. Lett. **81**, 742 (1998).
- [17] J. Werner, A. Griesmaier, S. Hensler, J. Stuhler, T. Pfau, A. Simoni, and E. Tiesinga, Phys. Rev. Lett. **94**, 183201 (2005).
- [18] L. Santos and T. Pfau, cond-mat/0510634.